Erschienen in: Environmental Microbiology ; 20 (2018), 12, S. 4369-4384
https://doi.org/10.1111/1462-2920.14356

Methanol metabolism in the acetogenic bacterium *Acetobacterium woodii*

Florian Kremp,[1] Anja Poehlein,[2] Rolf Daniel[2] and Volker Müller[1*]

[1]*Department of Molecular Microbiology and Bioenergetics, Institute of Molecular Biosciences, Johann Wolfgang Goethe University, Max-von-Laue Str. 9, D-60438, Frankfurt, Germany.*

[2]*Göttingen Genomics Laboratory, Institute for Microbiology and Genetics, Georg August University, Grisebachstr. 8, D-37077, Göttingen, Germany.*

Summary

Methanol derived from plant tissue is ubiquitous in anaerobic sediments and a good substrate for anaerobes growing on C_1 compounds such as methanogens and acetogens. In contrast to methanogens little is known about the physiology, biochemistry and bioenergetics of methanol utilization in acetogenic bacteria. To fill this gap, we have used the model acetogen *Acetobacterium woodii* to study methanol metabolism using physiological and biochemical experiments paired with molecular studies and transcriptome analysis. These studies identified the genes and enzymes involved in acetogenesis from methanol and the redox carriers involved. We will present the first comprehensive model for carbon and electron flow from methanol in an acetogen and the bioenergetics of acetogenesis from methanol.

Introduction

Acetogenic bacteria are characterized by a special pathway for carbon dioxide reduction to acetate, the Wood–Ljungdahl pathway (WLP), that is used for anabolism as well as catabolism (Drake, 1994). It is the only pathway of carbon dioxide fixation that is coupled to the synthesis of ATP and thus considered to be ancient and, if not the first biochemical pathway on earth (Martin, 2011; Poehlein *et al*., 2012; Sousa *et al*., 2013). The pathway involves reduction of CO_2 to formic acid, binding of formic acid to the C_1 carrier tetrahydrofolic acid (THF) and subsequent reduction of the formyl group to methyl-THF. In the second branch of the pathway another CO_2 is reduced to CO by the CO dehydrogenase/acetyl-CoA synthase (CODH/ACS) and then the methyl group, CO and CoA are condensed by the CODH/ACS to acetyl-CoA (Wood *et al*., 1986; Schuchmann and Müller, 2014). The WLP is also well suited for the conversion of other one carbon (C_1) substrates such as carbon monoxide (Diender *et al*., 2015), formate (Balch *et al*., 1977), formaldehyde (Schink, 1994) or methanol (Bache and Pfennig, 1981) that enter the WLP by different routes. Carbon monoxide and formate are intermediates of the WLP. Formaldehyde reacts spontaneously with THF to yield methylene-THF (Kallen and Jencks, 1966), also an intermediate of the WLP. Methanol could in principle be oxidized by a methanol dehydrogenase to formaldehyde, that then enters the WLP, or the methyl group could be transferred to THF by a methyltransferase system yielding methyl-THF. Whereas the former pathway is usually found in aerobic methylotrophs (Chistoserdova *et al*., 2009), the latter is usually found in anaerobes. Methyltransferase systems normally contain three different proteins (or sometimes three different domains present in two proteins): a methyltransferase I (MTI) that transfers the methyl group to a corrinoid protein (CoP) and a second methyltransferase (MTII) that transfers the methyl group from methyl-CoP to an acceptor, CoM in methanogens or THF in acetogens (Van der Meijden *et al*., 1983a,b; Kreft and Schink, 1994). The methyltransferase systems involved in methanol (and methylamine) metabolism of methanogenic archaea have been identified biochemically and studied to a great extent (Van der Meijden *et al*., 1983a,b, 1984b; Burke and Krzycki, 1995, 1997; Sauer *et al*., 1997; Sauer and Thauer, 1997; Hagemeier *et al*., 2006). The genes encoding the methanol-dependent methyltransferase systems are also known: *mtaB* codes for MTI, *mtaC* for the CoP and *mtaA* for the MTII. In contrast there are only a few reports on methyltransferase systems of acetogens acting on methanol (Van der Meijden *et al*., 1984a; Stupperich and Konle, 1993; Das *et al*., 2007; Visser *et al*., 2016). Growth on methanol has been described for an uncharacterized acetogen (Hamlett and Blaylock, 1969),

Received 29 May, 2018; accepted 7 July, 2018. *For correspondence. E-mail vmueller@bio.uni-frankfurt.de; Tel. +49-69-79829507; Fax: +49-69-79829306.

Butyribacterium methylotrphicum (Lynd and Zeikus, 1983), *Acetobacterium woodii* (Bache and Pfennig, 1981), *Moorella thermoacetica* (Daniel *et al*., 1990), *Eubacterium limosum* (Van der Meijden *et al*., 1984b) and *Sporomusa* species (Möller *et al*., 1984). Zhou and colleagues purified a corrinoid protein enriched during growth on methanol (Zhou *et al*., 2005). Its N-terminal amino acid sequence identified *mtaC* as the encoding gene, and next to *mtaC* the genes *mtaB* and a gene with similarity to methyl-THF MT of several bacteria were found (Das *et al*., 2007). *Sporomusa ovata* also produces a corrinoid protein during growth on methanol (Stupperich *et al*., 1992) that transfers the methyl group to THF (Stupperich and Konle, 1993). Recently, using a proteome approach a methyltransferase system consisting of MtaB, MtaC and a methyl-THF MT (with analogous function to MtaA of methanogens) was identified in *Sporomusa ovata* strain An4 (Visser *et al*., 2016). However, acetogenic bacteria can not only use the methyl group of methanol but also of methyl chloride or phenyl methyl ethers such as vanillate or veratrol (Messmer *et al*., 1993; Kaufmann *et al*., 1998; Naidu and Ragsdale, 2001; Siebert *et al*., 2005; Drake *et al*., 2006), and the methyltransferases catalysing *O*-demethylation of veratrol and vanillate have been identified and characterized. The MTI is the enzyme that confers substrate specificity to the methyltransferase systems and the MTI proteins of the vanillate and veratrol methyltransferase systems of *Acetobacterium dehalogenans* (OdmB and VdmB) are only 23% identical to each other (Studenik *et al*., 2012). With the MTI of the methanol methyltransferase system of the methanogen *Methanosarcina barkeri* (Sauer *et al*., 1997) they share identity values lower than 10% only.

The acetogenic bacterium *A. woodii* is currently the best biochemically understood acetogen. However, nothing is known about the pathway that allows the entry of the methyl group to the WLP and neither the further metabolism of the methyl group nor the nature of the redox carriers involved are known. Therefore, the aim of this work was to identify the methanol-dependent methyltransferase system and to establish the genes and enzymes participating in acetogenesis from methanol and the redox carriers involved in the model acetogen *A. woodii.*

Results

Growth of A. woodii on methanol

Cells transferred from a fructose-grown preculture transferred into the same complex medium containing 60 mM methanol showed a lag phase of 45 h before growth started (Fig. 1A), indicating the induction of genes required for methanol metabolism. Growth occurred with a doubling time of 16 h to a final OD of 1.5, but growth rate as well as final OD increased upon continuous subculturing on methanol. Final OD and growth rate was depending on the methanol concentration with a maximum at 60 mM methanol. Thereafter, growth rates decreased and the maximal concentration of methanol tolerated was 900 mM (Fig. 1B).

Transcriptome analyses of cells grown on methanol

To identify proteins/genes involved in methanol metabolism, cells were grown in complex medium with 60 mM methanol and samples were taken at an OD of 0.6. RNA extraction, cDNA synthesis and transcriptome analyses were performed as described in materials and methods. The most strongly expressed genes were Awo_c22810-Awo_c22740 with a LOG_2 of the fold change between 9.5 up to 14 compared with growth on fructose (Table 1). These eight genes are clustered on the chromosome and are transcribed in the same direction, with Awo_c22810 being the first.

Properties of methanol utilization genes and deduced proteins

The gene cluster Awo_c22810-Awo_c22740, comprising eight genes, extends over 6737 bp. Between Awo_c22780 and Awo_c22770 there is an intergenic region with a length of 240 bp which is remarkable within this cluster and may be a region for transcriptional regulation of the following genes Awo_c22770-Awo_c22740. A putative hairpin forming transcriptional terminator was found at the end of the cluster, 30 bp downstream of Awo_c22740 (5′-AUAACGAUAAAGCCGGCAUUAUGUGCCGGCUUUAUUGCGGGCA-3′). The free energy of the putative secondary structure is −14.5 kcal/mol (−59 kJ/mol).

Awo_c22810 codes for a putative regulator, homologous to PocR of *Salmonella thyphimurium* (Table 2). The derived amino acid sequence of Awo_c22800 showed high degree of identity to a corrinoid protein known from dimethylamine metabolism of methanogens. The predicted protein of Awo_22790 is homologous to YeiR and CobW and, therefore, seems to be involved in cobalamin biosynthesis. BLASTp algorithm based search did not reveal any homologous protein for the predicted amino acid sequence of Awo_c22780. Anyway, the C-terminus harbours a high number of histidine residues which are known to be important for metal-binding, therefore, the protein could be involved in cobalt-binding, -storage or -delivery. Translation of Awo_c22770 leads to an amino acid sequence with a predicted B_{12}-binding domain. The part of the gene cluster discussed before might be important for the biosynthesis of cobalamin, whereas the next genes might encode the methyltransferase system.

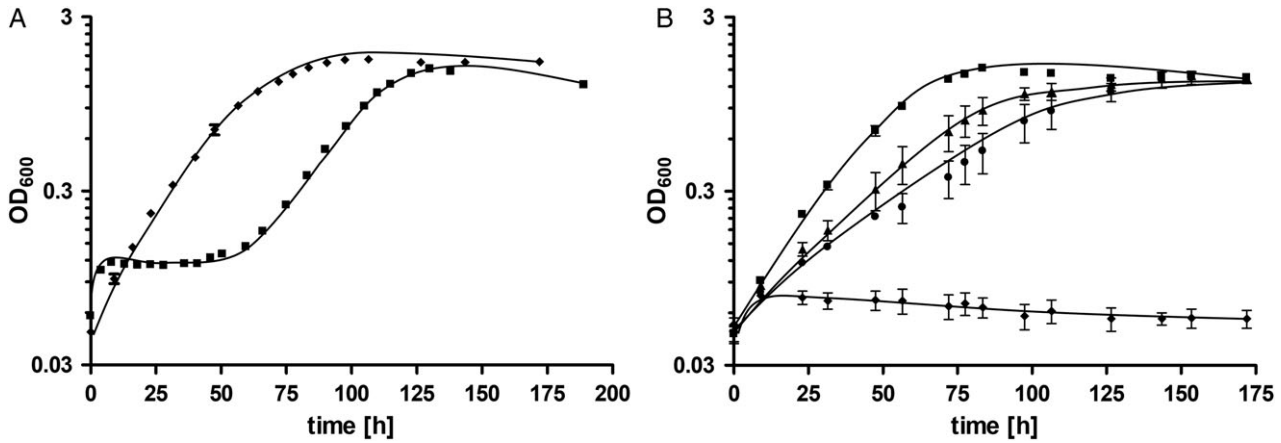

Fig. 1. Growth of *A. woodii* on methanol. A. Adaption of *A. woodii* to growth on methanol. Carbonate-buffered complex medium according to Heise and colleagues (1989) was supplemented with methanol (60 mM) and inoculated with *A. woodii* precultures grown on fructose (■) or methanol (♦). Growth was followed by measuring the optical density at 600 nm. B. Effect of increasing methanol concentration on growth of *A. woodii*. Media were inoculated to an optical density of 0.05 with a preculture grown on 60 mM methanol. The methanol concentration was 0.06 (■), 0.75 (▲), 0.90 (●) or 1.35 M (♦) respectively.

Awo_c22760 encodes a MTI, Awo_c22750 codes for a corrinoid protein and the derived amino acid sequence of Awo_c22740 is similar to methyl-THF:CoP methyltransferases (MTII). Therefore Awo_c22760-Awo_c22740 most likely encode the methanol methyltransferase system of *A. woodii.* As it was already recognized for *M. thermoacetica* and *S. ovata* strain An4 the MTII of *A. woodii* shares no similarity to a methyl-CoP:CoM methyltransferase (MTII) known to be involved in the methanol metabolism of methanogens (Das *et al*., 2007; Visser *et al*., 2016), but this is not too surprising since the acceptor molecules CoM and THF are quite different. Based on the high homology to the methanol utilization clusters of other acetogenic bacteria and methanogenic archaea, the gene cluster Awo_c22810-c22740 is further named *mta* cluster of *A. woodii.*

The methanol utilization genes are transcribed in a polycistronic message

To analyse whether the methanol utilization genes are organized in an operon, mRNA was isolated from *A. woodii* grown on methanol and transcribed into cDNA. This cDNA was then used as a template in a PCR reaction using primers (Supporting Information Table S1) that bridge the intergenic regions between *mtaR*/*mtaC1, mtaC1*/*W, mtaW*/*X, mtaX*/*Y, mtaY*/*B, mtaB*/*C2* and *mtaC2*/*A* as indicated in Fig. 2A. Only a cDNA originating from one polycistronic mRNA is able to give products with the expected fragment sizes of 778, 653, 743, 648, 688, 909 and 851 bp respectively. As can be seen from Fig. 2B, all of the expected PCR products were obtained. Use of corresponding mRNA as template yielded no PCR products. This result demonstrates that *mtaR, mtaC1, mtaX, mtaW, mtaY, mtaB, mtaC2* and *mtaA* constitute an operon. While the genes *mtaR-mtaY* may play a role in regulation and the synthesis of cobalamin, the gene products of *mtaB, mtaC2* and *mtaA* most likely are involved in the transfer of methyl groups to THF.

The methyl group is oxidized to CO_2 via the reverse WLP

Next we tested for the presence of the WLP in methanol-grown cells. Except the strongly induced gene cluster Awo_c22810-Awo_c22740 ($2^{9.5}$–2^{14} times higher transcript abundance compared with fructose grown cells, Table 1) the formyl-THF synthetase (Awo_c09260), formyl-THF cyclohydrolase (Awo_c09270) and the CODH/ACS cluster (Awo_c10670-Awo_c10760) were similar in transcript abundance. The methylene-THF dehydrogenase (Awo_c09280) and the methylene-THF reductase (Awo_c09290-Awo_c09310) were also similar in transcript level, as well as their activities in cell extracts from fructose- or methanol-grown cells (11.9/12.7 U/mg; 2.6/2.4 U/mg). Whereas the transcript level of the *rnf* genes (Awo_c22010-Awo_c22060) did not show a significant change, the activity changed from 12 mU/mg in fructose-grown cells to 80 mU/mg in methanol-grown cells. The bifurcating hydrogenase (Awo_c26970-Awo_c27010) and the hydrogen-dependent CO_2 reductase (HDCR; Awo_c08190-Awo_c8260) were less abundant in methanol grown cells and the activity of the HDCR was slightly decreased from 7.4 in fructose grown cells to 3.0 U/mg in methanol grown cells. Cell free extracts also produced H_2 from formate, as catalysed by the HDCR. With a specific activity of 68 mU/mg, 7.9 μmol of H_2 were produced within 10 min. The electron bifurcating hydrogenase was present in methanol grown cells, as determined immunological, to provide reduced ferredoxin. In addition,

Table 1. Absolute and relative transcript abundance of key enzymes involved in methanol metabolism of *A. woodii*. The colour gradient (red-yellow-green) indicates low, moderate and high values of absolute transcript abundance and their fold change. Down- (red) and upregulation (green) are indicated by $\log_2$ (FC).

			growth on fructose			growth on methanol						
locus tag	**genetic context**	**annotation**	**replictae 1**	**replicate 2**	**replicate 3**	**replictae 1**	**replicate 2**	**replicate 3**	**fold change**	**$\log_2$ (FC)**	**likelihood**	**FDR**
Awo_c05040	thioredoxin	trx	13997	18683	16069	159295	139498	168369	9.58	3.26	1.00	0.00
Awo_c07520	MT cluster	methyltransferase 2 MttA2	173	156	113	5853	3983	3852	30.97	4.95	1.00	0.00
Awo_c07530	MT cluster	choline/carnitine/betaine transporter OpuD2	163	203	169	8880	5518	4947	36.16	5.18	1.00	0.00
Awo_c07540	MT cluster	methyltransferase 1 MttB10	262	305	157	10599	7144	6150	33.00	5.04	1.00	0.00
Awo_c07550	MT cluster	corrinoid protein MttC6	228	254	406	7330	5754	6029	21.52	4.43	1.00	0.00
Awo_c07560	MT cluster	choline/carnitine/betaine transporter OpuD3	213	235	262	1039	885	817	3.86	1.95	1.00	0.00
Awo_c08190	HDCR cluster	formate dehydrogenase FdhF1	359	363	337	126	87	105	3.33	-1.74	1.00	0.00
Awo_c08200	HDCR cluster	hydrogenase, Fe-S subunit HycB1	113	116	117	32	28	35	3.64	-1.86	1.00	0.00
Awo_c08210	HDCR cluster	formate dehydrogenase FdhF2	32093	34027	25881	3739	3445	3598	8.53	-3.09	1.00	0.00
Awo_c08230	HDCR cluster	hydrogenase Fe-S subunit HycB2	4998	5058	3222	797	740	719	5.89	-2.56	1.00	0.00
Awo_c08240	HDCR cluster	formate dehydrogenase accessory protein FdhD	3070	2788	3628	315	282	258	11.09	-3.47	1.00	0.00
Awo_c08250	HDCR cluster	hydrogenase Fe-S subunit HycB3	2851	2935	2522	254	230	216	11.87	-3.57	1.00	0.00
Awo_c08260	HDCR cluster	iron hydrogenase HydA2	9412	10197	7601	891	727	790	11.30	-3.50	1.00	0.00
Awo_c09260	Formyl-THF synthetase	Fhs1	5026	5050	3558	7144	4925	4692	1.23	0.30	1.00	0.00
Awo_c09270	Formyl-THF cyclohyd.	FchA	7524	6514	5212	9228	7097	6484	1.18	0.24	1.00	0.00
Awo_c09280	MTHFDH	FolD	12524	11595	10698	18014	14414	13661	1.32	0.40	1.00	0.00
Awo_c09290	MTHFR	RnfC2	33291	32668	24286	50984	36368	33754	1.34	0.42	1.00	0.00
Awo_c09300	MTHFR	MetV	8357	8162	8872	15122	11732	11256	1.50	0.59	1.00	0.00
Awo_c09310	MTHFR	MetF	21174	19829	16621	49828	40842	37888	2.23	1.16	1.00	0.00
Awo_c10670	CODH/ACS cluster	CODH Ni^{2+}-insertion accessory protein CooC1	7496	6669	7696	4914	4056	4149	1.67	-0.74	1.00	0.00
Awo_c10680	CODH/ACS cluster	corrinoid activation/regeneration protein	12793	11956	14904	18924	15921	15508	1.27	0.34	0.86	0.01
Awo_c10690	CODH/ACS cluster	hypothetical protein	4007	3385	4801	8278	6511	6889	1.78	0.83	0.98	0.00
Awo_c10700	CODH/ACS cluster	hypothetical protein	2623	2049	3096	4945	4533	4247	1.77	0.82	0.99	0.00
Awo_c10710	CODH/ACS cluster	CFeS protein, SSU AcsD	82773	73124	51564	64759	54075	48899	1.24	-0.31	1.00	0.00
Awo_c10720	CODH/ACS cluster	CFeS protein, LSU AcsC	68432	66636	58248	62387	48428	44375	1.25	-0.32	1.00	0.00
Awo_c10730	CODH/ACS cluster	methyltransferase 2	60691	55580	52302	56321	46555	46665	1.13	-0.17	1.00	0.00
Awo_c10740	CODH/ACS cluster	CODH, catalytic subunit AcsA	42686	38938	26515	90371	69079	59937	2.03	1.02	1.00	0.00
Awo_c10750	CODH/ACS cluster	CODH Ni^{2+}-insertion accessory protein CooC2	10989	9842	7058	30294	21624	18805	2.54	1.34	1.00	0.00
Awo_c10760	CODH/ACS cluster	ACS, catalytic subunit AcsB	51469	52211	48765	154622	132712	116199	2.65	1.40	1.00	0.00
Awo_c22010	Rnf cluster	electron transport complex protein RnfB	11657	11293	12033	25957	22789	21397	2.01	1.00	0.99	0.00
Awo_c22020	Rnf cluster	electron transport complex protein RnfA	4199	3803	2220	5418	3656	3616	1.24	0.31	0.55	0.04
Awo_c22030	Rnf cluster	electron transport complex protein RnfE	4700	5107	3007	6425	4630	4064	1.18	0.24	0.51	0.05

			growth on fructose			growth on methanol						
locus tag	**genetic context**	**annotation**	**replictae 1**	**replicate 2**	**replicate 3**	**replictae 1**	**replicate 2**	**replicate 3**	**fold change**	**log_2 (FC)**	**likelihood**	**FDR**
Awo_c22040	Rnf cluster	electron transport complex protein RnfG	5130	5408	4019	7583	5473	5545	1.28	0.35	0.98	0.00
Awo_c22050	Rnf cluster	electron transport complex protein RnfD	7456	7659	6020	8231	5826	5419	1.09	-0.12	0.97	0.00
Awo_c22060	Rnf cluster	electron transport complex protein RnfC1	12284	12423	10954	13753	10414	10228	1.04	-0.05	0.99	0.00
Awo_c22740	MeOH operon	methyltransferase 2 MtaA	36	44	33	667610	564403	621426	16402.12	14.00	1.00	0.00
Awo_c22750	MeOH operon	corrinoid protein MtaC2	4	17	22	214827	175734	183064	13340.12	13.70	1.00	0.00
Awo_c22760	MeOH operon	methyltransferase 1 MtaB	31	34	23	454242	343408	367273	13237.76	13.69	1.00	0.00
Awo_c22770	MeOH operon	hypothetical B12-binding protein MtaY	9	2	13	125321	121238	143130	16237.04	13.99	1.00	0.00
Awo_c22780	MeOH operon	hypothetical protein MtaX	17	38	48	55510	54298	61034	1658.66	10.70	1.00	0.00
Awo_c22790	MeOH operon	cobalamin biosynthesis CobW-like MtaW	25	21	11	22727	18677	20221	1081.14	10.08	1.00	0.00
Awo_c22800	MeOH operon	corrinoid Protein MtaC1	27	20	17	20545	17132	17856	867.70	9.76	1.00	0.00
Awo_c22810	MeOH operon	transcriptional regulator AraC family MtaR	77	61	67	51797	47741	50118	730.03	9.51	1.00	0.00
Awo_c23710	MT cluster	corrinoid protein MttC22	679	665	548	6384	5427	5905	9.36	3.23	1.00	0.00
Awo_c23720	MT cluster	transcriptional regulator AraC family	785	849	1157	5826	4822	5281	5.71	2.51	1.00	0.00
Awo_c23730	MT cluster	methyltransferase 1 MttB20	423	584	373	31296	25632	27476	61.16	5.93	1.00	0.00
Awo_c23740	MT cluster	corrinoid protein MttC23	220	299	175	11876	9121	10078	44.78	5.48	1.00	0.00
Awo_c23750	MT cluster	methyltransferase 2 MttA8	351	489	329	12513	9320	9586	26.88	4.75	1.00	0.00
Awo_c23760	MT cluster	hypothetical protein	212	305	315	7514	6351	6655	24.66	4.62	1.00	0.00
Awo_c23770	MT cluster	cobalamin biosynthesis CobW-like	170	266	257	6526	5843	6138	26.71	4.74	1.00	0.00
Awo_c26970	bif. hydrogenase	iron hydrogenase HydA1	57984	61263	46049	8405	6482	7128	7.51	-2.91	1.00	0.00
Awo_c26980	bif. hydrogenase	iron hydrogenase HydB	48702	48882	28932	4948	3539	3815	10.28	-3.36	1.00	0.00
Awo_c26990	bif. hydrogenase	iron hydrogenase HydD	10760	11716	12668	1220	928	994	11.19	-3.48	1.00	0.00
Awo_c27000	bif. hydrogenase	sensory transduction histidine kinase HydE	12054	12498	8415	1280	926	884	10.67	-3.42	1.00	0.00
Awo_c27010	bif. hydrogenase	iron hydrogenase HydC	17677	16786	15022	1636	1325	1426	11.28	-3.50	1.00	0.00

Table 2. Properties of methanol utilization genes and deduced proteins.

Accession no./name	Length (bp)	Predicted mass (kDa)	Conserved motifs/domains	Homologous proteins	Identity[a] (%)	References
Awo_c22810/*mtaR*	1329	51.0	PocR sensory-/HTH-DNA-binding domain	PocR of *Salmonella typhimurium*	38	Bobik and colleagues (1992)
Awo_c22800/*mtaC1*	675	24.0	B_{12}-binding (DxHxxG)	MtbC2 (CoP) *Methanosarcina mazei*	38	Drennan and colleagues (1994); Kratzer and colleagues (2009)
Awo_c22790/*mtaW*	633	23.9	P-loop NTPase, Walker A and Walker B motif	YeiR of *E. coli*	31	Blaby-Haas and colleagues (2012)
				CobW of *Spromusa ovata* (predicted)	31	
				CobW of *Pseudomonas denitrificans*	28	Crouzet and colleagues (1991)
Awo_c22780/*mtaX*	471	18.3	None, high number of Histidin residues in C-terminus characteristic for metal binding	None	none	Cheng and colleagues (2013)
Awo_c22770/*mtaY*	393	14.4	B_{12}-binding domain	None	none	
Awo_c22760/*mtaB*	1395	50.5	Conserved cysteinyl- and glutamyl residues for Zn^{2+} binding, TIM-barrel	MtaB (MTI) of *Moorella thermoacetica*	57	Hagemeier and colleagues (2006)
				MtaB (MTI) of *S. ovata*	55	Visser and colleagues (2016)
				MtaB (MTI) *Methanosarcina barkeri*	37	Van der Meijden et al. (1984b)
Awo_c22750/*mtaC2*	639	22.7	B_{12}-binding domain (DxHxxG)	MtaC (CoP) of *M. thermoacetica*	56	Das and colleagues (2007); Drennan and colleagues (1994)
				MtaC (CoP) of *S. ovata*	41	Visser and colleagues (2016)
				MtbC (CoP) of *M. barkeri*	44	Ferguson and colleagues (2000)
				MtaC (CoP) of *M. barkeri*	31	Sauer and colleagues (1997); Sauer and Thauer (1997)
Awo_c22740/*mtaA*	801	29.4	Pterin-binding domain	Methyl-THF:CoP methyltransferase (MTII) of *M. thermoacetica*	53	Das and colleagues (2007)
				Methyl-THF:CoP methyltransferase (MTII) of *S. ovata*	43	Visser and colleagues (2016)

[a]Identity on protein level was identified by using BLASTp algorithm.

CO dehydrogenase as well as the formyl-tetrahydrofolate synthetase could also be identified immunologically (Supporting Information Fig. S1). In sum, these data are in accordance with the assumption that the methyl group is oxidized *via* a reversal of the WLP.

Purification of the methylene-THF reductase from methanol-grown cells

After transfer of the methyl group to THF, part of the methyl-THF has to be oxidized to CO_2 to generate electrons for the reduction of CO_2 to CO which condenses with another part of methyl-THF and CoA to acetyl-CoA. Oxidation of methyl-THF with NAD^+ as oxidant is a highly endergonic reaction ($\Delta G_0' = 23$ kJ/mol) and represents a steep energetic barrier in the methyl group oxidation pathway. In the reverse direction, the reaction is highly exergonic and it was speculated to be involved in energy conservation (Thauer *et al*., 1977). Since the enzyme harbours two flavin binding sites (one in MetF and RnfC2 respectively), the discovery of flavin-based electron bifurcation (Buckel and Thauer, 2018) led to the idea that this mechanism may be used to reduce ferredoxin that is then re-oxidized in the respiratory chain to give additional ATP. The reverse, electron confurcation with a strong reducing agent could then drive the endergonic methyl-THF

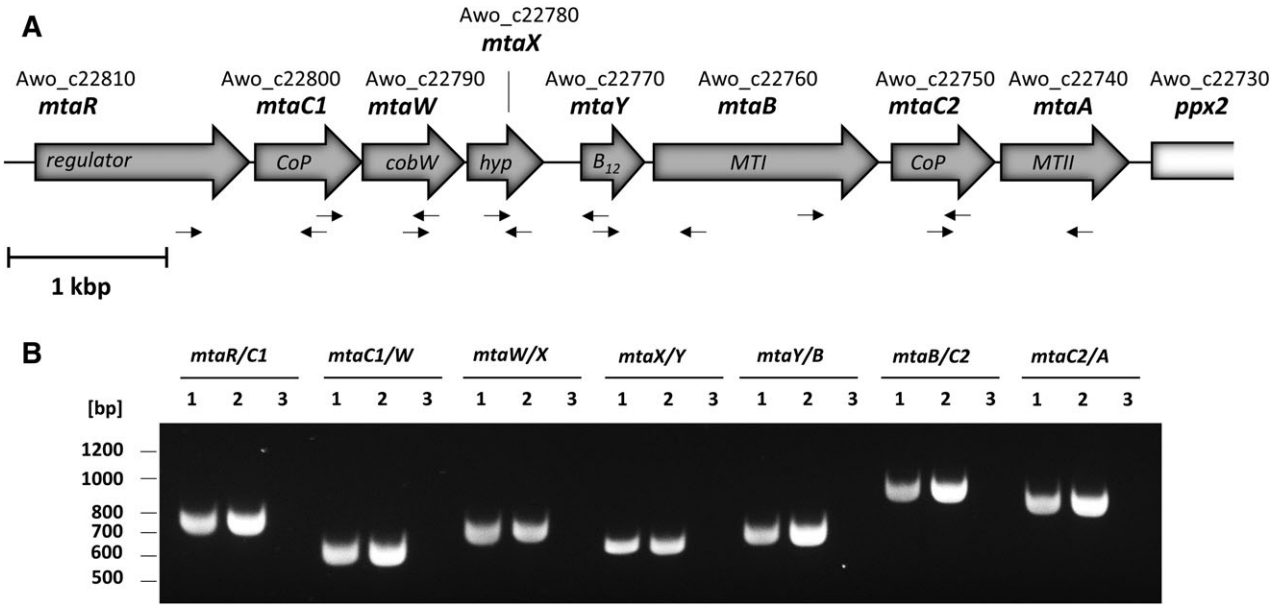

Fig. 2. Arrangement and expression analysis of *mta* genes in *A. woodii*. The *mta* operon of *A. woodii* comprises eight genes. B. For operon analysis total RNA from *A. woodii* was prepared and the contaminating DNA was removed. cDNA was synthesized by reverse transcriptase. To analyse the transcriptional unit cDNA was used as template for PCR to bridge the intergenic regions of the *mta* genes (lane 2). Genomic DNA and RNA were used as positive and negative controls respectively (lanes 1, 3). Oligonucleotides used in this study are listed in Supporting Information Table S1 and their location is indicated by black arrows in panel A.

oxidation. To address the biochemistry and energetics of methyl-THF oxidation, the methylene-THF reductase (MTHFR) was purified from methanol-grown cells essentially as described before for cells grown on fructose (Bertsch *et al*., 2015). Using 35 g of wet cells, the enzyme was purified 66.5-fold from cytoplasmic fraction via Q-Sepharose, Phenyl-Sepharose, Sephacryl S300 and Blue-Sepharose (Supporting Information Table S2). The purified

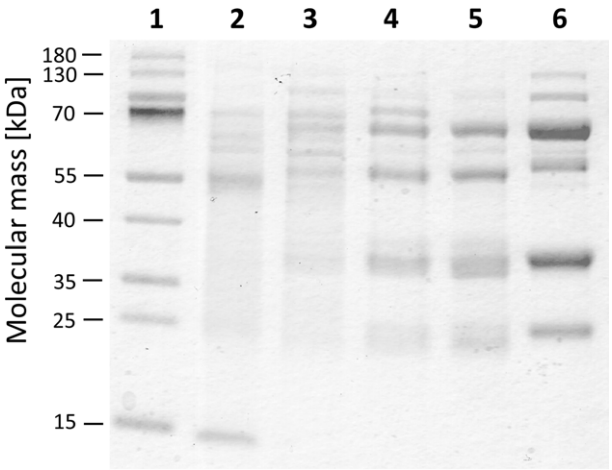

Fig. 3. Purification of the methylene-THF reductase of *A. woodii*. About 10 μg protein samples from the different purification steps were separated by SDS-PAGE. The proteins were stained with Coomassie Brilliant Blue. Lane 1, protein ladder; lane 2, cytoplasm; lane 3, pooled fractions from Q-Sepharose; lane 4, pooled fractions from Phenyl-Sepharose; lane 5, pooled fractions from Sephacryl S300; lane 6, pooled fractions from Blue-Sepharose.

enzyme catalysed the methylene-THF-dependent oxidation of NADH with an average activity of 286 U/mg and contained three major proteins with an apparent molecular mass of 70, 31 and 23 kDa respectively (Fig. 3), matching the expected mass of the MTHFR subunits RnfC2, MetF and MetV (71, 33, 23 kDa). One major contaminating protein (54 kDa) was identified as glycine tRNA-ligase by MALDI-TOF analysis. As a control, the MTHFR was also purified from fructose-grown cells. The enzyme had the same molecular mass and catalysed methylene-THF-dependent oxidation of NADH with an activity of 259 U/mg of protein. Apparently, the MTHFR from methanol- and fructose-grown cells had the same subunit composition.

When measured in the standard buffer (50 mM MOPS, pH 7, 10 mM NaCl, 20 mM $MgSO_4$, 4 μM reaszurin, 2 mM DTE), the methyl-THF dependent NAD^+ reduction by MTHFR could not be detected, but addition of an aliquot of cytoplasm to the assay enabled clear NAD^+ reduction, as described before for the enzyme purified from fructose-grown cells (Bertsch *et al*., 2015). This was interpreted to be caused by the removal of the product of the reaction by the subsequent enzymes of the pathway. The transcriptome analyses revealed the proteinaceous electron carrier thioredoxin (Awo_c05040) to be overproduced 10-fold during growth on methanol (Table 1). To address whether this thioredoxin is involved in methyl-THF oxidation, the gene was cloned and expressed in *E. coli* and the protein was purified to apparent homogeneity by affinity chromatography (Supporting Information Fig. S2A). The heterologously produced thioredoxin was

nearly completely oxidized (95%–97%) but could be fully reduced with 1,4-Dithiothreitol (DTT). It was catalytically active in reducing insulin with electrons derived from DTT (Supporting Information Fig. S2B). However, reduced thioredoxin did not stimulate methyl-THF-dependent NAD^+ reduction catalysed by the MTHFR of *A. woodii.* Reduced ferredoxin also did not stimulate the reaction. Interaction of the MTHFR with ferredoxin may require electron-transferring flavoproteins. The genome of *A. woodii* encodes two different EtfAB pairs, one in the context of the electron-bifurcating caffeyl-CoA reductase CarCDE (Bertsch *et al*., 2013) and one in the context of the electron bifurcating lactate dehydrogenase LctBCD (Weghoff *et al*., 2015). Neither one of these was expressed during growth on methanol nor did the addition of purified CarDE stimulate methyl-THF:NAD^+ oxidoreductase reaction. The inability of the enzyme to catalyse detectable oxidation of methyl-THF coupled to NAD^+ reduction could simply reflect the unfavourable equilibrium of the reaction. Assuming concentrations of 0.2 mM for methyl-THF and 1 mM for NAD^+ only ~ 0.4% of the added NAD^+ would be reduced to NADH.

Oxidation of methyl-THF to methylene-THF according to:

$$\text{methyl-THF} + \text{NAD}^+ \rightarrow \text{methylene-THF} + \text{NADH} + \text{H}^+ \quad \left(\Delta G_0' = 23\,\text{kJ/mol}\right)$$

produces a proton. Therefore, methyl-THF oxidation should be 'pulled' by low proton concentrations in order to make NADH production detectable. This was indeed observed. As can be seen in Fig. 4, increasing pH values stimulated methyl-THF oxidation. There was no activity at pH 5.5, but activity linearly increased with increasing pH up to the maximum at pH 8.5, whereafter activity declined slightly. Divalent cations such as magnesium and calcium but also chloride anion increased the methyl-THF:NAD^+ oxidoreductase activity by up to 100%. The same was observed with MTHFR purified from fructose-grown cells. To further characterize the enzyme, substrate affinities were determined. The dependence of the activity on methyl-THF and NAD^+ concentrations was hyperbolic with saturation at 0.8 and 1 mM, respectively, and K_m values of 86 and 165 μM (Fig. 5A and B).

Discussion

We have identified here by a transcriptome approach the genes involved in methanol conversion in the model acetogen *A. woodii.* The gene cluster encodes for MTI (MtaB), CoP (MtaC) and MTII (MtaA). The genes are highly expressed during growth on methanol, they have high identity values compared with predicted and verified methanol methyltransferase systems of methanogens and acetogens like the genes from *M. barkeri*, *S. ovata* or *M. thermoacetica.* Furthermore, the genetic arrangement is similar to other methyltransferase systems coding clusters. Thus, we hypothesize that they constitute the methanol-specific methyltransferase system of *A. woodii.* In addition to these, five more genes are encoded in the operon. They may have a role in regulation and biosynthesis of the corrinoid cofactor. These genes, in the same order, are also present in *Eubacterium limosum* (similarity on amino acid level: *mtaR* 70%; *mtaC1* 68%; *mtaW* 63%; *mtaX* 38%; *mtaY* 42%; *mtaB* 71%; *mtaC2* 69%; *mtaA* 77%; Fig. 6). *Acetobacterium dehalogenans* lacks *mtaY.* In *Sporomusa ovata* the genes have been shuffled around and *mtaW* and *mtaX* are at the end of the cluster. *Moorella thermoacetica* lacks the biosynthesis genes. In addition the order of the genes encoding MTI, MTII and CoP is different in *S. ovata* and *M. thermoacetica* (Das *et al*., 2007; Pierce *et al*., 2008; Visser *et al*., 2016). These data

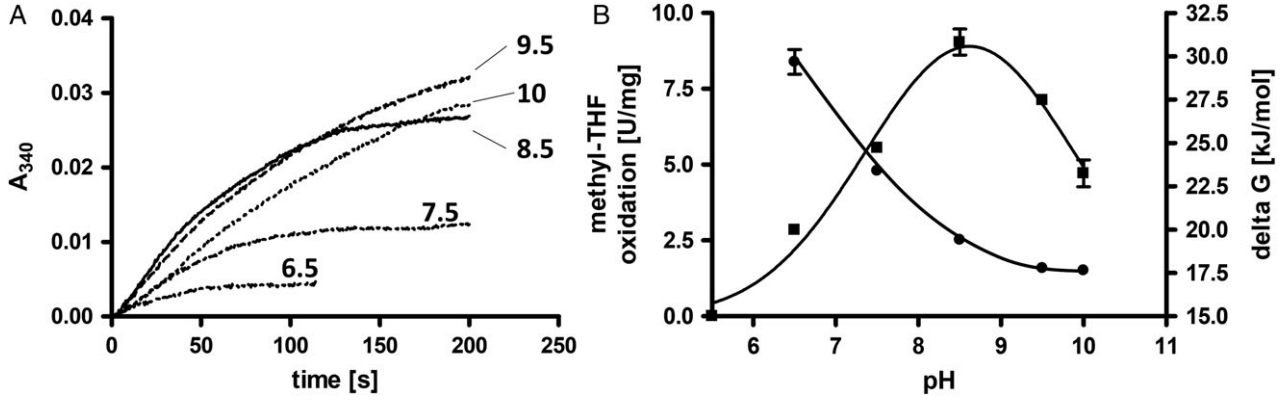

Fig. 4. pH optimum of methyl-THF:NAD^+ oxidoreductase activity. The methyl-THF dependent reduction of NAD^+ was measured by following the absorbance at 340 nm in combined buffer II with 10 μM FMN, 0.2 mM methyl-THF and 1 mM NAD^+. A. After the measurement was started by addition of MTHFR (0.6 μg) to the assay NAD^+ reduction was observed by following the absorbance at 340 nm in combined buffer II with different pH values as indicated. B. pH profile of methyl-THF oxidation (■) and pH dependence of the free energy change (●).

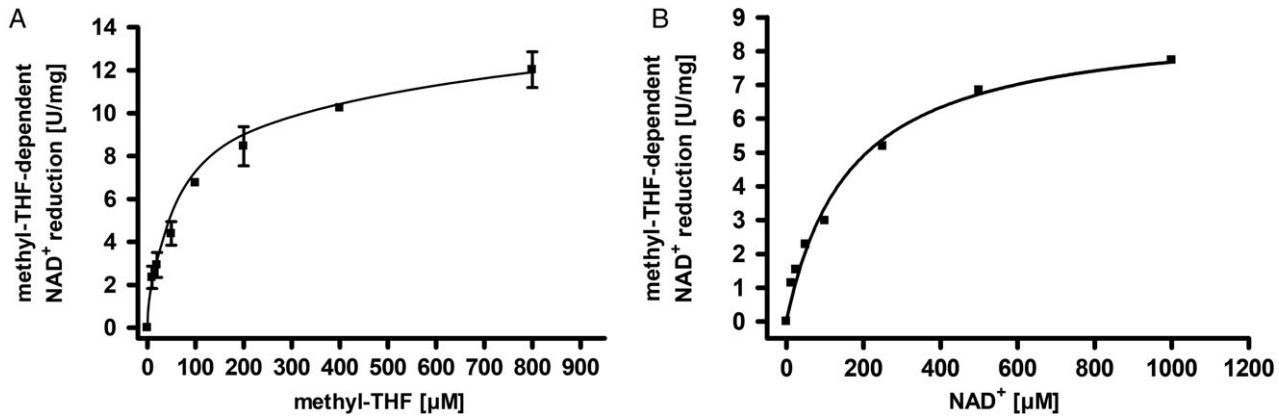

Fig. 5. Substrate dependence of methyl-THF oxidation. The methyl-THF-dependent reduction of NAD^+ was measured in 50 mM Tris buffer (pH 8.5) containing 10 mM NaCl, 20 mM $MgSO_4$, 2 mM DTE with 10 µM FMN and different concentrations of either methyl-THF (**A**) or and NAD^+ (**B**). The protein concentration was 0.6 µg ml^{-1}. Curve fitting and determination of the kinetic parameters K_m and V_{max} were performed using the GraphPad Prism program (version 4.03) and the Michaelis–Menten equation [$Y = (V_{max} \times X)/(K_m + X)$].

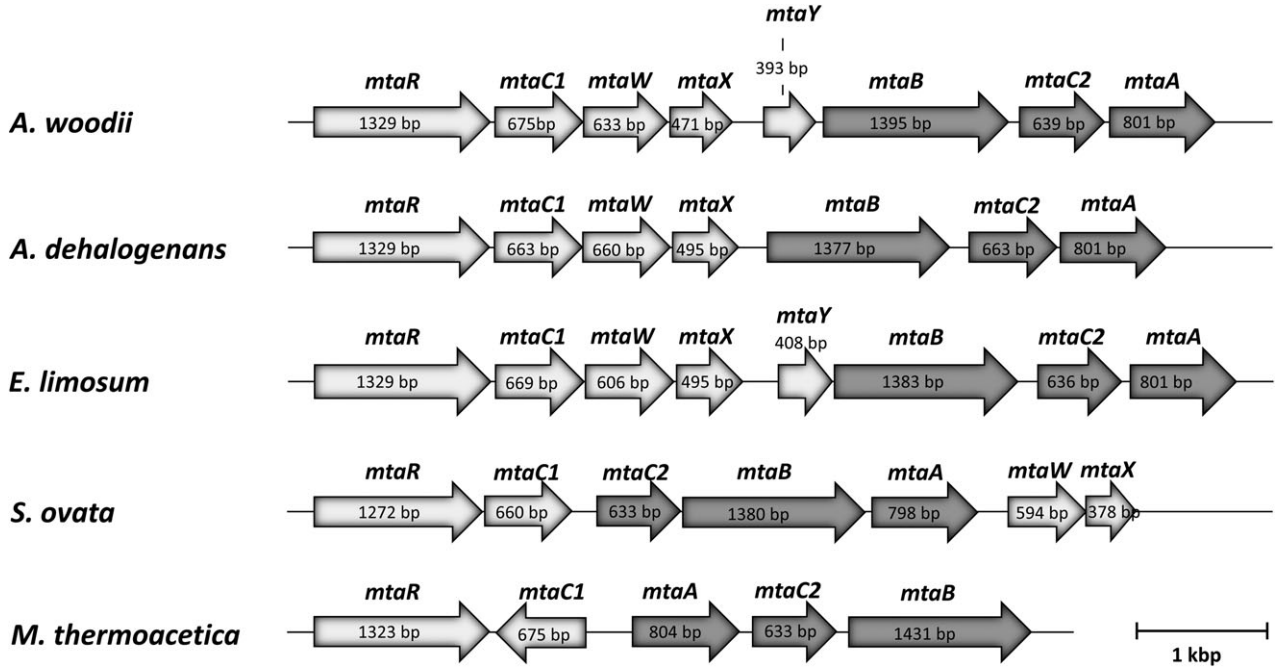

Fig. 6. Organization of potential *mta* operons within acetogenic bacteria. Use of the derived amino acid sequence of the MTII coding gene of *A. woodii* (Awo_c22740) for BLAST searches revealed potential *mta* operons. *A. dehalogenans* DSM 11527 (A3KSDRAFT_01004-A3KSDRAFT_00998), *E. limosum* KIST612 (ELI_1997-ELI_2005), *S. ovata* H1, DSM 2662 (SOV_3c00500-SOV_3c00430) and *M. thermoacetica* ATCC 39073 (Moth_1205-Moth_1209).

implicate that these gene clusters encode the methanol-specific methyltransferases of *A. dehalogenans*, *E. limosum*, *S. ovata* and *M. thermoacetica.* The biosynthesis genes are located somewhere else in the genome in *M. thermoacetica.* In addition to those shown in Fig. 6 similar gene clusters were found in *Acetobacterium bakii*, *Eubacterium callanderi*, *Eubacterium aggregans*, *Sporomusa sphaeroides*, *Sporomusa acidovorans*, *Sporomusa malonica* and *Moorella mulderi.*

The genome of *A. woodii* encodes ~ 30 different methyltransferase systems (Poehlein *et al*., 2012) of which Awo_c22760-Awo_c22740 had the highest transcript level in methanol-grown cells (Table 1). MTI of *A. woodii* did show some reasonable identity to MtaB of *M. thermoacetica*, *S. ovata* and *M. barkeri* but no recognizable identity to vanillate-specific MTI of *A. dehalogenans* and *M. thermoacetica* or to the veratrol-specific MTI of *A. dehalogenans* (Table 3).

Table 3. Comparison of the methanol:THF methyltransferase system to phenyl ether cleavage systems of *A. dehalogenans* and *M. thermoacetica*.

A. woodii genes	Gene	Function	Metabolism	Organism	Length (bp)	Identity[a] (%)	Accession no.	References
mtaB (1395 bp)	*odmB*	MTI	Vanillate	*A. dehalogenans*	981	none	AAC83696	Kaufmann and colleagues (1998)
mtaC2 (639 bp)	*odmA*	CoP			630	45	AAC83695	
mtaA (801 bp)	*odmD*	MTII			804	35	AAR11880	
mtaB (1395 bp)	*vdmB*	MTI	Veratrol	*A. dehalogenans*	966	none	AAQ89566	Engelmann and colleagues (2001); Siebert and colleagues (2005)
mtaC2 (639 bp)	*vdmA*	CoP			630	42	AAQ89565	
mtaA (801 bp)	*vdmD*	MTII			807	34	AAQ89564	
mtaB (1395 bp)	*mtvB*	MTI	Vanillate	*M. thermoacetica*	1170	none	Moth_0386	Naidu and Ragsdale (2001)
mtaC2 (639 bp)	*mtvC*	CoP			624	38	Moth_0387	
mtaA (801 bp)	*mtvA*	MTII			798	35	Moth_0385	

[a]identity on protein level were identified by using BLASTp algorithm.

This reflects the very different substrates used by the MTI's. Further the question arises why Awo_c7520-Awo_c7560 and Awo_c23710-Awo_c23770, both also potentially encoding methyltransferase systems, were also induced in methanol-grown cells (Table 1). At least for Awo_c07520-Awo_c07560 the question can be answered. Cells were grown on methanol in yeast extract containing medium. Yeast extract contains glycine betaine (GB) and *A. woodii* can grow on glycine betaine. Indeed, Awo_c07520-Awo_c07560 encode the glycine betaine-specific methyltransferase system (Lechtenfeld *et al*., 2018). Apparently, *A. woodii* can use methanol and GB simultaneously, but not fructose and GB. Since the putative MTI Awo_c23730 is only 9% identical to the MTI of the methanol methyltransferase system (Awo_c22760) it is unlikely that Awo_c23710-Awo_c23770 encodes a second methyltransferase system acting on methanol. The identity of 11% to the MTI of the GB-utilizing cluster is too low as well. Sequence alignments with the methyltransferases VdmB and OdmB reveal identity values of 30% and 25% respectively. From these findings we assume that Awo_c23710–23770 is a gene cluster coding for a methyltransferase system acting on an unknown substrate. Nevertheless, the reason for the enhanced transcription of this gene cluster in methanol-grown cells remains elusive, but we speculate that this compound is present in yeast extract.

From the data presented we hypothesize that methyl-THF is the product of the methyltransferase activity. Oxidation of one methyl group yields six reducing equivalents (=6 electrons) that can be used to reduce 3 mol of CO_2 to CO. The presence of the enzymes of the WLP was demonstrated immunologically as well as by activity measurements indicating that the oxidation of methyl groups is *via* reversal of the WLP. Hydrogen production alongside acetate formation was demonstrated. Since the methylene-THF reductase and the methylene-THF dehydrogenase in *A. woodii* are NAD^+ dependent and the HDCR produces H_2 (Schuchmann and Müller, 2013; Kottenhahn *et al*., 2018), the soluble electron bifurcating hydrogenase and the membrane bound Rnf complex are required for redox balancing, that is, conversion of 2.5 mol NADH and 1 mol of H_2 to 3 mol reduced ferredoxin required for CO_2 reduction according to

$$H_2 + 0.5\,NAD^+ + 0.5\,Fd \rightarrow 1.5\,H^+ + 0.5\,NADH + 0.5\,Fd^{2-}$$

$$2.5\,NADH + 5\,Na^+{}_{out} + 2.5\,Fd \rightarrow$$

$$2.5\,NAD^+ + 2.5\,H^+ + 5\,Na^+{}_{in} + 2.5\,Fd^{2-}.$$

The electrochemical Na^+ potential, required to drive Fd reduction, is generated by ATP hydrolysis. This is not without precedence but observed before in ethanol (Bertsch *et al*., 2016) and lactate metabolism (Weghoff *et al*., 2015) in *A. woodii*.

A critical reaction in methyl group oxidation is the oxidation of methyl-THF to methylene-THF, as catalysed by the methylene-THF reductase. The reaction catalysed in the oxidative direction is highly endergonic and flavin-based electron bifurcation (FBEB) was discussed as one mechanism to drive this reaction with reduced ferredoxin as co-reductant. We had purified the enzyme before from fructose-grown cells of *A. woodii* and found no indication for electron bifurcation (Bertsch *et al*., 2015). The same was found for the enzyme purified from methanol-grown cells. It catalysed methyl-THF oxidation with NAD^+ as oxidant and ferredoxin (oxidized or reduced) did not affect the reaction. Thioredoxin from *A. woodii* also did not affect the reaction. The reactions following methyl group oxidation pull the first one. This notion is in accordance with the fact that addition of cytoplasmic fraction to MTHFR stimulates methyl-THF oxidation. The same was observed by addition of enriched methylene-THF dehydrogenase (Bertsch *et al*., 2015). Thus, we conclude that the electron flow in the methyl branch of the WLP involves only NADH and H_2. This allows to present a comprehensive model for

the electron and carbon flow during acetogenesis from methanol and its bioenergetics (Fig. 7). Oxidation of the methyl group yields one ATP by substrate level phosphorylation (SLP) in the formyl-tetrahydrofolate synthetase reaction. Three additional mol of ATP are generated in the acetate kinase reaction. Of those 4 mol of ATP, 1.5 have to be invested to export the sodium ions required for ferredoxin reduction by the Rnf complex. This leaves 2.5 mol of ATP for the cells to grow:

$$4\,CH_3OH + 2\,CO_2 + 2.5\,ADP + 2.5\,P_i \rightarrow$$
$$3\,CH_3COOH + 2.5\,ATP + 2\,H_2O$$

This is equivalent to 0.83 ATP per mol of acetate, the largest ATP gain reported so far for an acetogenic C_1 substrate and the second largest after fructose (0.3 for H_2 + CO_2 (Schuchmann and Müller, 2014); 0.25 for lactate (Weghoff *et al*., 2015); 0.37 for ethanol (Bertsch *et al*., 2016); 0.47 for butanediol (Hess *et al*., 2015); 0.62 for ethylene glycol (Trifunovic *et al*., 2016) and 1.4 for fructose (Schuchmann and Müller, 2016)). The high ATP yield is in accordance to high cell yields (MeOH: 10 g/mol acetate; H_2 + CO_2: 4.2 g/mol acetate; (Bache and Pfennig, 1981; Tschech and Pfennig, 1984). Methanol is another 'low energy' substrate that can be used only with the help of the two redox balancing mechanisms: the soluble FBEB and membrane-bound reverse electron transport. They enable the electron transfer from NADH and H_2 to ferredoxin, which is required for CO_2 reduction in the carbonyl branch of the WLP.

Experimental procedures

Cultivation of A. woodii

A. woodii DSMZ 1030 was routinely cultivated at 30 °C in the medium described previously (Heise *et al*., 1989, 1992). Methanol (60 mM) or fructose (20 mM) was used as growth substrate. Growth was monitored by measuring the optical density at 600 nm (OD_{600}).

RNA-seq analysis

Harvested cells were resuspended in 800 µl RLT buffer (RNeasy Mini Kit, Qiagen) with β-Mercaptoethanol (10 µl ml^{-1}) and cell lysis was performed using a laboratory ball mill. Subsequently 400 µl RLT buffer (RNeasy Mini Kit Qiagen) with β-Mercaptoethanol (10 µl ml^{-1}) and 1200 µl 96% [v/v] ethanol were added. For RNA isolation, the RNeasy Mini Kit (Qiagen) was used as recommended by the manufacturer, but instead of RW1 buffer RWT buffer (Qiagen) was used in order to isolate RNAs smaller 200 nt also. To determine the RNA integrity number (RIN) the isolated RNA was run on an Agilent Bioanalyzer 2100 using an Agilent RNA 6000 Nano Kit as recommended by the manufacturer (Agilent Technologies, Waldbronn, Germany). Remaining genomic DNA was removed by digesting with TURBO DNase (Invitrogen, ThermoFischer Scientific, Paisley, United Kingdom). The Ribo-Zero magnetic kit (Epicentre Biotechnologies, Madison, WI) was used to reduce the amount of rRNA-derived sequences. For sequencing, the strand-specific cDNA libraries were constructed with a NEBNext Ultra

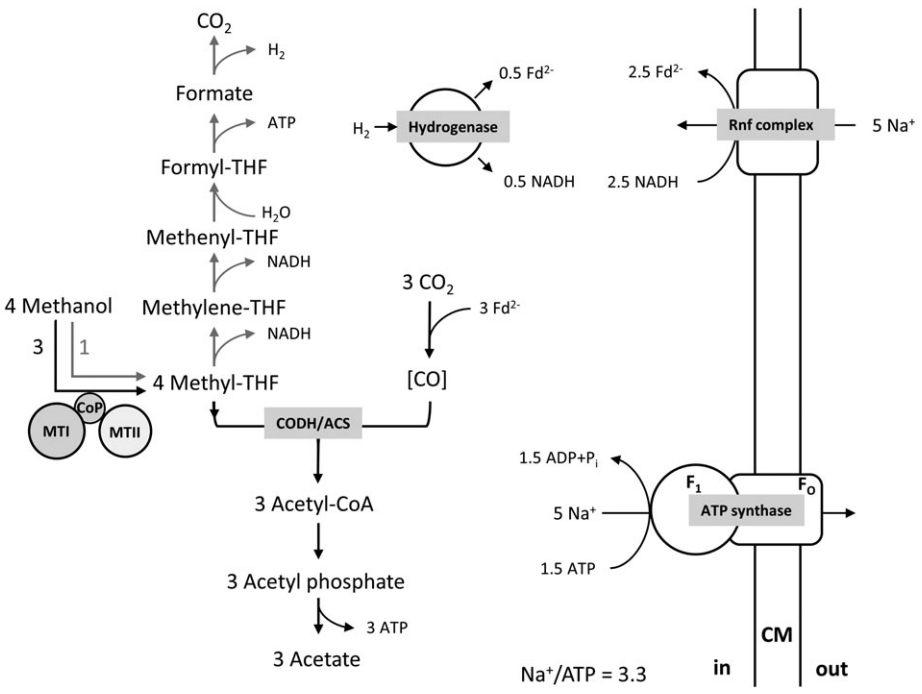

Fig. 7. Carbon and electron flow in methanol metabolism of *A. woodii*. In order to generate electrons for CO_2 reduction one of four methyl groups has to be oxidized in the methyl branch of WLP. The bifurcating hydrogenase as well as the Rnf complex are used for redox balancing of NADH and Fd. Therefore, a reverse Na^+ flow, energized by ATP hydrolysis, is required.

directional RNA library preparation kit for Illumina (New England BioLabs, Frankfurt am Main, Germany) and sequenced by using the Genome Analyser IIx instrument (Illumina Inc., San Diego, CA) using the Genome Analyser SBS kit v3 in the paired-end mode and running 2× 112 cycles. Between 12 980 600 and 27 592 992 raw reads were generated for the samples (for details see Supporting Information Table S3). For quality filtering and removing of remaining adaptor sequences, Trimmomatic-0.32 (Bolger *et al*., 2014) and a cutoff phred-33 score of 15 were used. The mapping of the remaining sequences was performed with the Bowtie (version 2) program (Langmead and Salzberg, 2012) using the implemented end-to-end mode, which requires that the entire read align from one end to the other. First, surviving paired end reads were mapped against a database consisting of tRNA and rRNA sequences of *A. woodii* and unaligned reads were subsequently mapped against the genome of *A. woodii.* Differential expression analyses were performed with the BaySeq program (Mortazavi *et al*., 2008). Genes with $\log_2$ fold change in expression of ≥2.0 or ≤−2.0, a likelihood value of ≥0.9, and an adjusted *p* value of ≤0.05 (the *p* value was corrected by the false discovery rate [FDR] on the basis of the Benjamini–Hochberg procedure) were considered differentially expressed. The RNA-seq data have been submitted to the SRA database.

RNA isolation and cotranscription analysis

Cells of *A. woodii* grown on methanol or fructose were harvested, resuspended in 10 mM Tris buffer (pH 8) containing 1 mM EDTA and 3 mg ml^{-1} lysozyme and incubated for 30 min at 37°C. After addition of 30 zirconoxide balls, the cells were disrupted in a MM 301 mixer mill (Retsch, Germany) at 30 Hz for 5 min. Total RNA was isolated from the extract using the InviTrap Spin Cell RNA Mini Kit (Stratec Molecular, Germany) according to the manufacturer's protocol. Remaining DNA contaminations were removed by addition of RQ1 DNase (Promega, Germany) in the presence of RNasin Plus RNase inhibitor (Promega, Germany) according to the manufacturer's protocols. Isolated RNA was stored at −80°C. cDNA synthesis was performed using the RNase H minus point mutant M-MLV reverse transcriptase (Promega, Germany) in the presence of RNasin Plus RNase inhibitor (Promega, Germany) according to the manufacturer's protocols.

The arrangement of the eight putative *mta* genes was analysed with PCR with cDNA as template, using 30 cycles. Chromosomal DNA and isolated RNA of *A. woodii* were used as positive and negative control. PCRs were performed as described previously (Sambrook *et al*., 1989). Primers used are listed in Supporting Information Table S1.

Purification of MTHFR

All buffers used for the purification of MTHFR contained 2 mM dithioerythritol (DTE) and 4 μM resazurin and all purification steps were performed under strictly anoxic conditions at room temperature in an anaerobic chamber (Coy Laboratory Products, USA) filled with 96% N_2 and 4% H_2. *A. woodii* was grown under anoxic conditions in 20-l flasks (Glasgerätebau Ochs, Germany) using methanol as substrate to an OD_{600} of ~ 1.8. The cells were harvested (~ 35 g wet weight) and washed in 25 mM Tris buffer (pH 7.5) containing 420 mM saccharose. The cells were resuspended in the same buffer and incubated in the presence of 10 mg ml^{-1} lysozyme for 1 h at 37 °C. The generated protoplasts were resuspended in purification buffer (50 mM Tris, 20 mM $MgSO_4$, 20% glycerol, pH 7.6) in the presence of 0.5 mM phenylmethylsulfonyl fluoride (PMSF) and 0.1 mg ml^{-1} DNase I and passed three times through a French pressure cell (110 MPa). Cell debris was removed by centrifugation at 24 000*g* for 40 min. Membranes were removed by centrifugation at 160 000*g* for 90 min. The purification of the MTHFR from the cytoplasm was performed as described previously (Bertsch *et al*., 2015).

Enzymatic activity assays

All measurements were performed in 1.8-ml anoxic cuvettes (Glasgerätebau Ochs, Germany) sealed by rubber stoppers under a N_2 atmosphere at 23 °C (except the determination of the temperature optimum). In all measurements the reduction or oxidation of NAD^+/NADH was followed at 340 nm (ε = 6.2 mM^{-1} cm^{-1}). Routinely, purification of the MTHFR was followed by measuring the oxidation of NADH (0.25 mM) in the presence of FMN (10 μM) and a racemic mixture of methylene-THF synthesized nonenzymatically with THF (0.5 mM) and formaldehyde (1.5 mM) in buffer I [50 mM 3-(N-Morpholino) propanesulfonic acid (pH 7)], 10 mM sodium chloride, 20 mM magnesium sulfate, 4 μM resazurin and 2 mM DTE). For the further characterization of the methyl-THF oxidation, methyl-THF (0.2 mM) and NAD^+ (1 mM) were used as substrates. The determination of the pH optimum was performed in a combined buffer II containing MES/-MOPS/Tris/CHES/CHAPS (25 mM each), sodium chloride (10 mM) and magnesium sulfate (20 mM). To determine the influence of ions on enzyme activity buffer III [Tris (pH 8.5)] was used, containing either 50 mM of magnesium sulfate, magnesium chloride, sodium chloride, potassium chloride or calcium chloride respectively.

To determine the methylene-THF dehydrogenase activity the reduction of 1 mM NAD^+ was followed using methylene-THF as substrate as described before (Bertsch *et al*., 2015). The HDCR activity was determined by following the reduction of methylviologen (10 mM) at 604 nm (ε = 13.9 mM^{-1} cm^{-1}) using formate (10 mM) as substrate as described (Schuchmann and Müller, 2013). Ferredoxin:NADH oxidoreductase (Rnf) activity was measured by following the reduction of NAD^+ (3 mM) using Fd_{red} [30 μM; purified from *Clostridium pasteurianum* and prereduced by CODH as described (Schönheit *et al*., 1978)] as electron donor. Methylene-THF dehydrogenase, HDCR and Rnf activity assays were performed in buffer I.

Determination of hydrogen and acetate

Cell free extracts were prepared from *A. woodii* cultures either grown on methanol or fructose to exponential growth phase. Cells were harvested under anoxic conditions and lysed as described already. Hydrogen was produced by cell extracts using 50 mM formate as substrate. To produce acetate, methanol was used as substrate either with H_2 + CO_2 (80:20 [v/v]) or N_2 + CO (70:30 [v/v]) as gas phase. The production assays were performed in 80 mM Bis(2-hydroxyethyl)amino-tris(hydroxymethyl) methan buffer (pH 6.8) containing, 10 mM $MgCl_2$, 10 mM NaCl, 2 mM DTE and 4 μM resazurin. Hydrogen and acetate concentrations were determined as described previously (Kottenhahn *et al*., 2018).

Heterologous expression of trx

Amplification of genes was done using Phusion DNA polymerase (New England BioLabs; Ipswich, MA) and genomic DNA of *A. woodii* as the template. After amplification, the genes were cloned into the HindIII and NdeI sites of pET21a and transformed into *Escherichia coli* DH5α. Constructs were verified *via* DNA sequencing and introduced into *E. coli* BL21(DE3). For expression, cells were grown at 37 °C to an OD of 0.6–0.8 and induced with 0.5 mM IPTG. The cells were harvested, washed with buffer W (100 mM Tris/HCl, 20 mM $MgSO_4$ 150 mM NaCl, 20% [vol/vol] glycerol, pH 8) and used immediately for purification.

Purification of Trx-Strep

Purification of Trx-Strep was performed under oxic conditions. Cells were resuspended in buffer W, DNaseI (0.1 mg ml^{-1}) and PMSF (0.5 mM) were added and the cells were disrupted in a French pressure cell (110 MPa). Cell debris was separated by centrifugation at 25 000*g* and 4 °C for 15 min. The cell free extract was loaded on a column containing 5 ml Strep-Tactin. The column was washed with 5 column volumes (CV) buffer W and eluted with 3 CV buffer E (100 mM Tris/HCl, 20 mM $MgSO_4$ 150 mM NaCl, 20% [vol/vol] glycerol, 5 mM desthiobiotin, pH 8). The protein was concentrated (Vivaspin 6, Cutoff 3 kDa, Sartorius Stedim Biotech GmbH, Göttingen) to a concentration of 9 mg/ml and its redox state was determined according to Ellman (1959). The DTT:insulin oxidoreductase activity of Trx was measured as described before (Holmgren, 1979).

Analytical methods

Protein concentration was measured according to Bradford (Bradford, 1976) Proteins were separated in 12% polyacrylamide gels according to Schägger and von Jagow (1987) and stained with Coomassie Brilliant Blue G250.

Acknowledgements

This project has received funding from the European Research Council (ERC) under the European Union's Horizon 2020 research and innovation programme (grant agreement no 741791).

References

Bache, R., and Pfennig, N. (1981) Selective isolation of *Acetobacterium woodii* on methoxylated aromatic acids and determination of growth yields. *Arch Microbiol*. **130**: 255–261.

Balch, W. E., Schoberth, S., Tanner, R. S., and Wolfe, R. S. (1977) *Acetobacterium*, a new genus of hydrogen-oxidizing, carbon dioxide-reducing, anaerobic bacteria. *Int J Syst Bact*. **27**: 355–361.

Bertsch, J., Parthasarathy, A., Buckel, W., and Müller, V. (2013) An electron-bifurcating caffeyl-CoA reductase. *J Biol Chem*. **288**: 11304–11311.

Bertsch, J., Öppinger, C., Hess, V., Langer, J. D., and Müller, V. (2015) A heterotrimeric NADH-oxidizing methylenetetrahydrofolate reductase from the acetogenic bacterium *Acetobacterium woodii*. *J Bacteriol*. **197**: 1681–1689.

Bertsch, J., Siemund, A. L., Kremp, F., and Müller, V. (2016) A novel route for ethanol oxidation in the acetogenic bacterium *Acetobacterium woodii*: the acetaldehyde/ethanol dehydrogenase pathway. *Environ Microbiol*. **18**: 2913–2922.

Blaby-Haas, C. E., Flood, J. A., Crecy-Lagard, V., and Zamble, D. B. (2012) YeiR: a metal-binding GTPase from *Escherichia coli* involved in metal homeostasis. *Metallomics*. **4**: 488–4897.

Bobik, T. A., Ailion, M., and Roth, J. R. (1992) A single regulatory gene integrates control of vitamin B_{12} synthesis and propanediol degradation. *J Bacteriol*. **174**: 2253–2266.

Bolger, A. M., Lohse, M., and Usadel, B. (2014) Trimmomatic: a flexible trimmer for illumina sequence data. *Bioinformatics*. **30**: 2114–2120.

Bradford, M. M. (1976) A rapid and sensitive method for the quantification of microgram quantities of protein utilizing

the principle of proteine-dye-binding. *Anal Biochem*. **72**: 248–254.

Buckel, W., and Thauer, R. K. (2018) Flavin-based electron bifurcation, ferredoxin, flavodoxin, and anaerobic respiration with protons (Ech) or NAD^+ (Rnf) as electron acceptors: a historical review. *Front Microbiol*. **9**: 1–24.

Burke, S. A., and Krzycki, J. A. (1995) Involvement of the 'a' isozyme of methyltransferase II and the 29-kilodalton corrinoid protein in methanogenesis from monomethylamine. *J Bacteriol*. **177**: 4410–4416.

Burke, S. A., and Krzycki, J. A. (1997) Reconstitution of monomethylamine:coenzyme M methyl transfer with a corrinoid protein and two methyltransferases purified from *Methanosarcina barkeri*. *J Biol Chem*. **272**: 16570–16577.

Chistoserdova, L., Kalyuzhnaya, M. G., and Lidstrom, M. E. (2009) The expanding world of methylotrophic metabolism. *Annu Rev Microbiol*. **63**: 477–499.

Cheng, T., Xia, W., Wang, P., Huang, F., Wang, J., and Sun, H. (2013) Histidine-rich proteins in prokaryotes: metal homeostasis and environmental habitat-related occurrence. *Metallomics*. **5**: 1423–1429.

Crouzet, J., Levy-Schil, S., Cameron, B., Cauchois, L., Rigault, S., Rouyez, M. C., *et al*. (1991) Nucleotide sequence and genetic analysis of a 13.1-kilobase-pair *Pseudomonas denitrificans* DNA fragment containing five *cob* genes and identification of structural genes encoding cob(I)alamin adenosyltransferase, cobyric acid synthase, and bifunctional cobinamide kinase-cobinamide phosphate guanylyltransferase. *J Bacteriol*. **173**: 6074–6087.

Das, A., Fu, Z. Q., Tempel, W., Liu, Z. J., Chang, J., Chen, L., *et al*. (2007) Characterization of a corrinoid protein involved in the C_1 metabolism of strict anaerobic bacterium *Moorella thermoacetica*. *Proteins*. **67**: 167–176.

Daniel, S. L., Hsu, T., Dean, S. I., and Drake, H. L. (1990) Characterization of the H_2-dependent and CO-dependent chemolithotrophic potentials of the acetogens *Clostridium thermoaceticum* and *Acetogenium kivui*. *J Bacteriol*. **172**: 4464–4471.

Diender, M., Stams, A. J., and Sousa, D. Z. (2015) Pathways and bioenergetics of anaerobic carbon monoxide fermentation. *Front Microbiol*. **6**: 1275.

Drake, H. L. (1994)Acetogenic bacteria . In *Acetogenesis*, Drake, H. L. (ed). New York: Chapman & Hall, pp. 14–25.

Drake, H. L., Küsel, K., and Matthies, C. (2006)Acetogenic prokaryotes . In *The Prokaryotes*, Dworkin, M., Falkow, S., Rosenberg, E., Schleifer, K.-H., and Stackebrandt, E. (eds). New York: Springer-Verlag, pp. 354–420.

Drennan, C. L., Huang, S., Drummond, J. T., Matthews, R. G., and Lidwig, M. L. (1994) How a protein binds B_{12}: a 3.0 a X-ray structure of B_{12}-binding domains of methionine synthase. *Science*. **266**: 1669–1674.

Ellman, G. L. (1959) Tissue sulfhydryl groups. *Arch Biochem Biophys*. **82**: 70–77.

Engelmann, T., Kaufmann, F., and Diekert, G. (2001) Isolation and characterization of a veratrol:corrinoid protein methyl transferase from *Acetobacterium dehalogenans*. *Arch Microbiol*. **175**: 376–383.

Ferguson, D. J., Jr., Gorlatova, N., Grahame, D. A., and Krzycki, J. A. (2000) Reconstitution of dimethylamine: coenzyme M methyl transfer with a discrete corrinoid protein and two methyltransferases purified from *Methanosarcina barkeri*. *J Biol Chem*. **275**: 29053–29060.

Hagemeier, C. H., Krer, M., Thauer, R. K., Warkentin, E., and Ermler, U. (2006) Insight into the mechanism of biological methanol activation based on the crystal structure of the methanol-cobalamin methyltransferase complex. *Proc Natl Acad Sci USA*. **103**: 18917–18922.

Hamlett, N. V., and Blaylock, B. A. (1969) Synthesis of acetate from methanol. *Bacteriol Proc*. **69**: 149.

Heise, R., Müller, V., and Gottschalk, G. (1989) Sodium dependence of acetate formation by the acetogenic bacterium *Acetobacterium woodii*. *J Bacteriol*. **171**: 5473–5478.

Heise, R., Müller, V., and Gottschalk, G. (1992) Presence of a sodium-translocating ATPase in membrane vesicles of the homoacetogenic bacterium *Acetobacterium woodii*. *Eur J Biochem*. **206**: 553–557.

Hess, V., Oyrik, O., Trifunovic, D., and Müller, V. (2015) 2,3-butanediol metabolism in the acetogen *Acetobacterium woodii*. *Appl Environ Microbiol*. **81**: 4711–4719.

Holmgren, A. (1979) Thioredoxin catalyzes the reduction of insulin disulfides by dithiothreitol and dihydrolipoamide. *J Biol Chem*. **254**: 9627–9632.

Kallen, R. G., and Jencks, W. P. (1966) The mechanism of the condensation of formaldehyde with tetrahydrofolic acid. *J Biol Chem*. **241**: 5851–5863.

Kaufmann, F., Wohlfarth, G., and Diekert, G. (1998) *O*-demethylase from *Acetobacterium dehalogenans*-substrate specificity and function of the participating proteins. *Eur J Biochem*. **253**: 706–711.

Kottenhahn, P., Schuchmann, K., and Müller, V. (2018) Efficient whole cell biocatalyst for formate-based hydrogen production. *Biotechnol Biofuels*. **11**: 93.

Kratzer, C., Carini, P., Hovey, R., and Deppenmeier, U. (2009) Transcriptional profiling of methyltransferase genes during growth of *Methanosarcina mazei* on trimethylamine. *J Bacteriol*. **191**: 5108–5115.

Kreft, J. U., and Schink, B. (1994) *O*-demethylation by the homoacetogenic anaerobe *Holophaga foetida* studied by a new photometric methylation assay using electrochemically produced cob(I)alamin. *Eur J Biochem*. **226**: 945–951.

Langmead, B., and Salzberg, S. L. (2012) Fast gapped-read alignment with bowtie 2. *Nat Methods*. **9**: 357–359.

Lechtenfeld, M., Heine, J., Sameith, J., Kremp, F., and Müller, V. (2018) Glycine betaine metabolism in the acetogenic bacterium *Acetobacterium woodii*. *Environ Microbiol*. doi: 10.1111/1462-2920.14389.

Lynd, L. H., and Zeikus, J. G. (1983) Metabolism of H_2-CO_2, methanol, and glucose by *Butyribacterium methylotrophicum*. *J Bacteriol*. **153**: 1415–1423.

Martin, W. F. (2011) Early evolution without a tree of life. *Biol Direct*. **6**: 36.

Messmer, M., Wohlfarth, G., and Diekert, G. (1993) Methyl chloride metabolism of the strictly anaerobic, methyl chloride-utilizing homoacetogen strain MC. *Arch Microbiol*. **160**: 383–387.

Möller, B., Oßmer, R., Howard, B. H., Gottschalk, G., and Hippe, H. (1984) *Sporomusa*, a new genus of gram-negative anaerobic bacteria including *Sporomusa sphaeroides* spec. Nov and *Sporomusa ovata* spec. Nov. *Arch Microbiol*. **139**: 388–396.

Mortazavi, A., Williams, B. A., McCue, K., Schaeffer, L., and Wold, B. (2008) Mapping and quantifying mammalian transcriptomes by RNA-Seq. *Nat Methods*. **5**: 621–628.

Naidu, D., and Ragsdale, S. W. (2001) Characterization of a three-component vanillate *O*-demethylase from *Moorella thermoacetica*. *J Bacteriol*. **183**: 3276–3281.

Pierce, E., Xie, G., Barabote, R. D., Saunders, E., Han, C. S., Detter, J. C., *et al*. (2008) The complete genome sequence of *Moorella thermoacetica* (f. *Clostridium thermoaceticum*). *Environ Microbiol*. **10**: 2550–2573.

Poehlein, A., Schmidt, S., Kaster, A.-K., Goenrich, M., Vollmers, J., Thürmer, A., *et al*. (2012) An ancient pathway combining carbon dioxide fixation with the generation and utilization of a sodium ion gradient for ATP synthesis. *PLoS One*. **7**: e33439.

Sambrook, J., Fritsch, E. F., and Maniatis, T. (1989) *Molecular Cloning: A Laboratory Manual*. Cold Spring Harbor, NY: Cold Spring Harbor Laboratory Press.

Sauer, K., and Thauer, R. K. (1997) Methanol:coenzyme M methyltransferase from *Methanosarcina barkeri* - zinc dependence and thermodynamics of the methanol:cob(I) alamin methyltransferase reaction. *Eur J Biochem*. **249**: 280–285.

Sauer, K., Harms, U., and Thauer, R. K. (1997) Methanol: coenzyme M methyltransferase from *Methanosarcina barkeri* - purification, properties and encoding genes of the corrinoid protein MT1. *Eur J Biochem*. **243**: 670–677.

Schägger, H., and von Jagow, G. (1987) Tricine-sodium dodecylsulfate-polyacrylamide gel electrophoresis for the separation of proteins in the range from 1 to 100 kDa. *Anal Biochem*. **166**: 369–379.

Schink, B. (1994)Diversity, ecology, and isolation of acetogenic bacteria . In *Acetogenesis*, Drake, H. L. (ed). New York: Chapman & Hall, pp. 197–235.

Schönheit, P., Wäscher, C., and Thauer, R. K. (1978) A rapid procedure for the purification of ferredoxin from clostridia using polyethylenimine. *FEBS Lett*. **89**: 219–222.

Schuchmann, K., and Müller, V. (2013) Direct and reversible hydrogenation of CO_2 to formate by a bacterial carbon dioxide reductase. *Science*. **342**: 1382–1385.

Schuchmann, K., and Müller, V. (2014) Autotrophy at the thermodynamic limit of life: a model for energy conservation in acetogenic bacteria. *Nat Rev Microbiol*. **12**: 809–821.

Schuchmann, K., and Müller, V. (2016) Energetics and application of heterotrophy in acetogenic bacteria. *Appl Environ Microbiol*. **82**: 4056–4069.

Siebert, A., Schubert, T., Engelmann, T., Studenik, S., and Diekert, G. (2005) Veratrol-*O*-demethylase of *Acetobacterium dehalogenans*: ATP-dependent reduction of the corrinoid protein. *Arch Microbiol*. **183**: 378–384.

Sousa, F. L., Thiergart, T., Landan, G., Nelson-Sathi, S., Pereira, I. A., Allen, J. F., *et al*. (2013) Early bioenergetic evolution. *Philos Trans R Soc Lond B Biol Sci*. **368**: 20130088.

Studenik, S., Vogel, M., and Diekert, G. (2012) Characterization of an *O*-demethylase of *Desulfitobacterium hafniense* DCB-2. *J Bacteriol*. **194**: 3317–3326.

Stupperich, E., and Konle, R. (1993) Corrinoid-dependent methyl transfer reactions are involved in methanol and 3,4-dimethoxybenzoate metabolism by *Sporomusa ovata*. *Appl Environ Microbiol*. **59**: 3110–3116.

Stupperich, E., Aulkemeyer, P., and Eckerskorn, C. (1992) Purification and characterization of a methanol-induced cobamide-containing protein from *Sporomusa ovata*. *Arch Microbiol*. **158**: 370–373.

Thauer, R. K., Jungermann, K., and Decker, K. (1977) Energy conservation in chemotrophic anaerobic bacteria. *Bact Rev*. **41**: 100–180.

Trifunovic, D., Schuchmann, K., and Müller, V. (2016) Ethylene glycol metabolism in the acetogen *Acetobacterium woodii*. *J Bacteriol*. **198**: 1058–1065.

Tschech, A., and Pfennig, N. (1984) Growth yield increase linked to caffeate reduction in *Acetobacterium woodii*. *Arch Microbiol*. **137**: 163–167.

Van der Meijden, P., Jansen, B., van der Drift, C., and Vogels, G. D. (1983a) Involvement of corrinoids in the methylation of coenzyme M (2-mercaptoethanesulfonic acid) by methanol and enzymes from *Methanosarcina barkeri*. *FEMS Microbiol Lett*. **19**: 247–251.

Van der Meijden, P., Heythuysen, H. J., Pouwels, A., Houwen, F., van der Drift, C., and Vogels, G. D. (1983b) Methyltransferases involved in methanol conversion by *Methanosarcina barkeri*. *Arch Microbiol*. **134**: 238–242.

Van der Meijden, P., van der Drift, C., and Vogels, G. D. (1984a) Methanol conversion in *Eubacterium limosum*. *Arch Microbiol*. **138**: 360–364.

Van der Meijden, P., te Brommelstroet, B. W., Poirot, C. M., van der Drift, C., and Vogels, G. D. (1984b) Purification and properties of methanol:5-hydroxybenzimidazolylcobamide methyltransferase from *Methanosarcina barkeri*. *J Bacteriol*. **160**: 629–635.

Visser, M., Pieterse, M. M., Pinkse, M. W., Nijsse, B., Verhaert, P. D., de Vos, W. M., *et al*. (2016) Unravelling the one-carbon metabolism of the acetogen *Sporomusa* strain An4 by genome and proteome analysis. *Environ Microbiol*. **18**: 2843–2855.

Weghoff, M. C., Bertsch, J., and Müller, V. (2015) A novel mode of lactate metabolism in strictly anaerobic bacteria. *Environ Microbiol*. **17**: 670–677.

Wood, H. G., Ragsdale, S. W., and Pezacka, E. (1986) The acetyl-CoA pathway of autotrophic growth. *FEMS Microbiol Rev*. **39**: 345–362.

Zhou, W., Das, A., Habel, J.E., Liu, Z.J., Chang, J., Chen, L. *et al*. (2005) Isolation, crystallization and preliminary X-ray analysis of a methanol-induced corrinoid protein from *Moorella thermoacetica*. *Acta Crystallogr Sect F Struct Biol Cryst Commun* **61**: 537–540.

Supporting Information

Additional Supporting Information may be found in the online version of this article at the publisher's web-site:

Fig. S1. Identification of enzymes of the WLP in cell free extracts of *A. woodii* grown on fructose and methanol. **A.** Separation of 10 μg protein of cell free extracts by SDS-PAGE. **B**. Detection of CO dehydrogenase (CODH), formyl-THF Synthetase (FTHFS) and the bifurcating hydrogenase (bif. hyd.) by immunological assays. 10 μg protein were separated in an SDS-PAGE and transferred to a nitrocellulose membrane.

Fig. S2. SDS-PAGE analysis and insulin reduction activity of Trx-Strep. **A.** Progress of the purification *via* Strep-Tactin.

Lane 1, flow through; lane 2 and 3, wash fractions; lane 4-9, eluted Trx-Strep. Per lane 15 µl protein fraction were separated. **B.** After DTT (0.33 mM) was added to 750 µg insulin in KP_i-buffer 10 µM of Trx-Strep catalyzed the precipitation of insulin.

Table S1. Oligonucleotides used in this study.

Table S2. Purification of the methylene-THF reductase of *A. woodii.*

Table S3. Details of transcriptomic analysis